RSC Advances

PAPER

View Article Online
View Journal | View Issue

Cite this: *RSC Adv.*, 2023, **13**, 16196

Controlling metal ion migration in contaminated groundwater with Iraqi clay barriers for water resource protection

Ayad A. H. Faisal, *[a] Zaid Abed Al-Ridah,[b] Nadhir Al-Ansari, [c] Waqed H. Hassan,[de] Osamah Al-Hashimi, [f] Ayman A. Ghfar[g] and Khalid Hashim [f]

Received 17th March 2023
Accepted 19th May 2023

DOI: 10.1039/d3ra01773g

rsc.li/rsc-advances

This study investigates the effectiveness of using Iraqi clay as a low-permeability layer to prevent the migration of lead and nickel ions in groundwater-aquifers. Tests of batch operation have been conducted to determine the optimal conditions for removing Pb^{2+} ions, which were found to be 120 minutes of contact time, a pH of 5, 0.12 g of clay per 100 mL of solution, and an agitation of 250 rpm. These conditions resulted in a 90% removal efficiency for a 50 mg L^{-1} initial concentration of lead ions. To remove nickel ions with an efficiency of 80%, the optimal conditions were 60 minutes of contact time, a pH of 6, 12 g of clay per 100 mL of solution, and an agitation of 250 rpm. Several sorption models were evaluated, and the Langmuir formula was found to be the most effective. The highest sorption capacities were 1.75 and 137 mg g^{-1} for nickel and lead ions, respectively. The spread of metal ions was simulated using finite element analysis in the COMSOL multiphysics simulation software, taking into account the presence of a clay barrier. The results showed that the barrier creates low-discharge zones along the down-gradient of the barrier, reducing the rate of pollutant migration to protect the water sources.

Introduction

The presence of heavy metals like lead, copper, nickel, and zinc in groundwater poses a significant threat to this vital resource,[1] particularly since 40% of global food production relies on irrigation from groundwater sources. Additionally, around two billion individuals rely on this water for drinking purposes.[2–5] In addition to natural sources of contamination, various human activities contribute to the release of diverse quantities and types of contaminants, including the use of pesticides, disposal of waste in sanitary landfill sites, storage of chemicals in underground tanks, application of contaminated soil, and transportation of chemical liquids.[6–10] It is very important to note that the infiltration of contaminants into the aquifer results in the formation of a distinctive plume, the migration of which is determined by the characteristics of the soil and the velocity of groundwater.[11] In several instances, the plume can intersect with wells that tap into the aquifer or emerge in surface water bodies, rendering the water sources unsafe for both human and wildlife consumption.[12,13] A commonly employed method for preventing the migration of contaminated water off-site is the utilization of a low permeability barrier (LPB). This technique involves the construction of an underground wall made of materials with low permeability coefficients and high swelling capacities. Soil-bentonite slurry and soil–cement–bentonite slurry are well-established types of LPBs, favored for their cost-effectiveness and ease of construction. LPBs can also serve as a funnel to redirect contaminated water towards the permeable reactive barrier for treatment.[14] Other forms of subsurface vertical barriers include grouted cut-off walls, sheet-pile walls, soil-mix barriers, and composite walls. The liner at the base of sanitary landfills can also act as an LPB and be part of the system used to collect leachate generated from water interaction with buried solid waste. The primary purpose of an LPB is to establish a low permeable structure in the soil to restrict groundwater flow and contain the transport of contaminants.[15–17] Numerous previous works have examined the efficacy of LPBs in restricting groundwater movement and, therefore, limiting the transport of contaminants in both real and simulated aquifers under various operational conditions.[18] Analytical solutions for calculating discharge and hydraulic head have been derived for steady groundwater flow in a two-

[a]*Department of Environmental Engineering, College of Engineering, University of Baghdad, Baghdad, Iraq. E-mail: ayad.faesal@coeng.uobaghdad.edu.iq*

[b]*College of Engineering, Al-Qasim Green University, Babylon, Iraq. E-mail: zaidalmnsory@yahoo.com*

[c]*Department of Civil, Environmental and Natural Resources Engineering, Lulea University of Technology, 97187 Lulea, Sweden. E-mail: nadhir.alansari@ltu.se*

[d]*College of Engineering, University of Warith Al-Anbiyaa, Kerbala, Iraq*

[e]*Department of Civil Engineering, College of Engineering, University of Kerbala, Kerbala 56001, Iraq. E-mail: waaqidh@uokerbala.edu.iq*

[f]*School of Civil Engineering and Built Environment, Liverpool John Moores University, Liverpool L3 3AF, UK. E-mail: O.A.AlHASHIMI@2020.ljmu.ac.uk; K.S.Hashim@ljmu.ac.uk*

[g]*Department of Chemistry, College of Science, King Saud University, P.O. Box 2455, Riyadh 11451, Saudi Arabia. E-mail: aghafr@ksu.edu.sa*

dimensional domain in the presence of an impermeable barrier. These solutions were designed to evaluate the containment of the source zone of pollution or the contaminant plume through the use of extraction wells and a vertical barrier.[16] A mixture of sand and regenerated bentonite, as well as natural clay, were tested as LPBs. The results showed that the combination of 90% sand and 10% industrial bentonite exhibited comparable geochemical and hydraulic properties to those of natural clay.[19] The restriction of kerosene movement in the two-dimensional unsaturated zone of sand was observed in the existence of clay barrier. Numerical simulator by finite difference approach was developed to describe the temporal and spatial distribution of oil saturation. The findings indicated that the clay lens played a crucial role in limiting the vertical flow of kerosene towards the groundwater table.[20] The utilization of geosynthetic clay as a liner in sanitary landfills to mitigate the migration of contaminants towards groundwater was investigated. The hydration of geosynthetic clay with varying initial water contents was analyzed in conjunction with clay subsoil under daily thermal cycles.[21] To predict the movement of cadmium ions in an aqueous solution, the COMSOL software was utilized within a tank filled with a bentonite/sand mixture as LPB (hydraulic conductivity coefficient of 1.98×10^{-10} m s^{-1}) sourced from the Kariman region of Sulaymaniyah Governorate, Iraq. The results indicated that the most effective configuration to safeguard a particular location is to surround it on three sides opposing the flow direction compared to a continuous barrier.[22] The use of commercial sorbents,[9,23–26] industrial wastes resulted as byproducts from various industries,[27–29] or manufacturing new valuable sorbents from these wastes[30–32] for elimination of chemicals from contaminated water is a crucial field that has studied recently. This study aims to utilize clay, an abundant and cost-effective material in the Iraqi environment, as an LPB to control the migration of lead and nickel ions through groundwater and protect water resources. This objective will be accomplished through an experimental program to determine the characteristics of clay and evaluate the migration of contaminants in a two-dimensional packed bed. The program of COMSOL Multiphysics version 3.5a has been used to calculate the velocity vector distribution and simulate the metal front based on the outcomes of the continuous tests.

Modeling of sorption data

Sorption is the relationship of the chemical retained onto sorbent (q_e) *versus* its concentration in the solution (C_e) at equilibrium. This relationship demonstrates that as the equilibrium concentration increases, the amount of adsorbed contaminant also increases, albeit not in a direct proportion. Six isotherm relationships were utilized for the analysis of sorption measurements, as outlined below:[33–35]

Langmuir model

This model assumes a surface with uniform adsorption energies and a lack of adsorbed transmigration in the surface plane, where:

$$q_e = \frac{q_m b C_e}{1 + b C_e} \quad (1)$$

where q_m is the largest capacity for sorption (mg g^{-1}) and b is the constant of saturation (L mg^{-1}).

Freundlich model

This model characterized by the following empirical formula:

$$q_e = K_F C_e^{1/n} \quad (2)$$

where K_F is the Freundlich equilibrium constant and n is an empirical constant referring to the sorption intensity.

Elovich model

Is characterized by multi-layer adsorption at which tremendous vacant sorption sites are evolved whenever adsorption is progressed:

$$\frac{q_e}{q_m} = C_e K_E \exp\left(-\frac{q_e}{q_m}\right) \quad (3)$$

where q_m is the Elovich ultimate sorption capacity (mg g^{-1}) and K_E is the Elovich constant (L mg^{-1}).

Temkin model

The adsorption in this model represents a uniform distribution of binding energies, reaching a maximum value. Also, the sorption heat of all molecules can decrease in a linear manner as the coverage of the sorbent surface increases. This model is expressed by the following equation:

$$\theta = \frac{RT}{\Delta Q} \ln K_o C_e \quad (4)$$

where θ is the partial coverage, R is the constant of gas (kJ mol^{-1} K^{-1}), T is the absolute temperature (K), ΔQ is the amount of sorption energy difference (kJ mol^{-1}), and K_o is the constant of Temkin (L mg^{-1}).

Kiselev model

Depicts the partitioning of the sorbate monolayer over the sorbent. It is considered somewhat valid when the surface coverage is approximately 68%. The Kiselev model is presented by eqn (5):

$$k_1 C_e = \frac{\theta}{(1-\theta)(1 + k_n \theta)} \quad (5)$$

where k_1 is the constant of Kiselev (L mg^{-1}) and θ is the fraction of the surface coverage.

Hill–de Boer model

It is described the mobile sorption as well as the lateral interactions induced among molecules as follows:

$$k_1 C_e = \frac{\theta}{1-\theta} \exp\left(\frac{\theta}{1-\theta} - \frac{k_2 \theta}{RT}\right) \quad (6)$$

where k_1 is the constant of Hill–de Boer (L mg^{-1}) and k_2 is an indicative constant to represent the extent of interactions among sorbet molecules (kJ mol^{-1}).

Experimental work

Materials

The Iraqi clay was utilized as a low-permeability barrier (LPB) and was obtained from the Iraqi Geological Survey-Ministry of Industry and Minerals. It is a powder with a bulk density of 1.114 g cm^{-3}, hydraulic conductivity of 6.5×10^{-8} cm s^{-1}, and porosity of 0.548. The clay has area of surfaces equal to 64 m^2 g^{-1}, with the following composition percentages: SiO_2 (52%), Al_2O_3 (16%), Fe_2O_3 (4.5%), CaO (5.7%), and MgO (3.5%). Natural Iraqi soil was used as the aquifer, with grain size in range (0.075–1.18 mm), median size of 0.43 mm, and uniformity coefficient of 1.85. The soil has a conductivity of 2.2×10^{-3} cm s^{-1}, porosity of 0.46, and bulk density of 1.39 g cm^{-3}, consisting primarily of 96.5% sand and 3.5% silt mixed with clay. To simulate groundwater contamination with heavy metals, lead and nickel were chosen. Lead nitrate (1.6 g) or nickel nitrate (4.6 g) were thoroughly dissolved in one litre of distilled water to create a stock solution with a metal content of 1000 mg L^{-1}. The acidity of the solution must modify as necessary by drops of 0.1 M HNO_3 or NaOH.

Batch study

Four stages in this study have achieved to specify the optimal conditions for removing contaminants. The following parameters were considered: initial contaminant concentration, initial pH, processing time, solid mass, and speed of agitation.

Stage one. At a specified initial lead or nickel concentration of 50 mg L^{-1}, different initial pH values (3–7) and times (≤180 min) were tested. A 0.12 g and 12 g sorbent were used for lead and nickel ions, respectively, with an agitation speed of 250 rpm.

Stage two. The clay dosage was varied from 0.025 to 12 g per 100 mL at the previously determined initial concentration and agitation speed to determine the best sorbent mass.

Stage three. Different initial contaminant concentrations (50 to 250 mg L^{-1} with a 50 mg L^{-1} increment) were examined with the best sorbent mass from stage two.

Stage four. Different agitation speeds (stationary to 250 rpm with a 50 rpm increment) were tested to determine the best speed at the initial contaminant concentration from stage three.

In each test, 100 mL of metal solution and a specified amount of clay were placed in 250 mL flasks and agitated using an orbital shaker. Specific volume (25 mL) is drawn from agitated solutions and clay isolated by Whatman No. 1 or Teknik No. 1 filter paper to measure the lead and nickel residuals. An aliquot of 15 mL of the clear filtrate was taken to measure the contaminant residuals using an "atomic absorption spectrophotometer (AAS, Sens AA, Australia)". The metal uptake (q_e) was calculated by eqn (7):[36]

$$q_e = (C_o - C_e)\frac{V}{m} \quad (7)$$

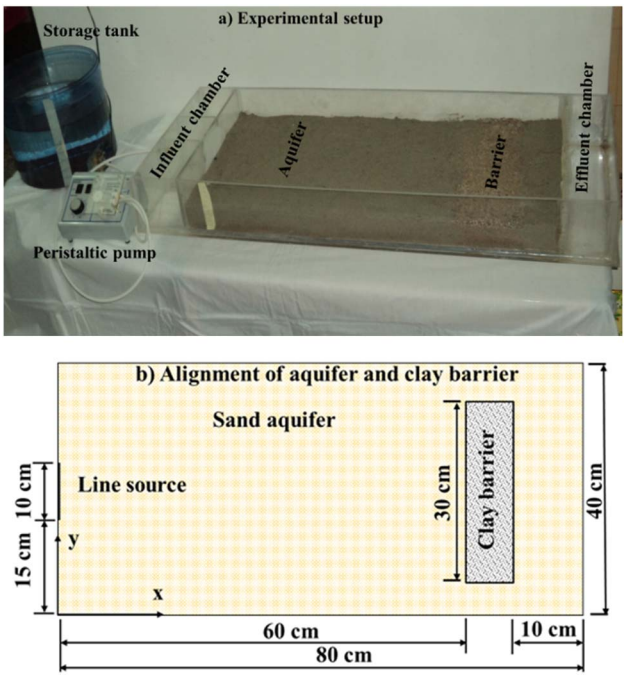

Fig. 1 Flow and contaminant transport domains (aquifer together with LPB) adopted in the present study.

where C_o is the initial contaminant concentration (mg L^{-1}), V is the effective volume of contaminant solution in each flask (L), and m is the reactive sorbent mass placed in each flask (g).

Continuous study. The transportation of simulated pollutants was conducted in a transparent bench-scale tank as shown in Fig. 1(a). This tank is constructed of rectangular acrylic glass with dimensions of 100 cm in length, 40 cm in width, and 10 cm in height. Two perforated filter partitions are provided to create a middle compartment, consisting of 60 cm × 40 cm × 5 cm of sandy soil, 10 cm × 40 cm × 5 cm of Iraqi clay, and 10 cm × 40 cm × 5 cm of sandy soil as illustrated schematically in Fig. 1(b). The two outer compartments served as control influent-effluent chambers to adjust the water table level in the middle zone and maintain it in a fully saturated state. A 100 L storage tank was used to supply the aquifer with a steady flow through pumping it by "peristaltic pump (Fisher Scientific, variable speed pump II-medium, model 3385, control company, USA)". Single sampling port was selected in the down-gradient of the Iraqi clay at coordinates (0.7 m, 0.2 m). Water samples were withdrawn at fixed intervals using syringes, and residual metals can measure by AAS.

Results and discussion

Effect of batch experimental parameters

Fig. 2 shows that longer contact time results in higher removal of Pb^{2+} and Ni^{2+} contaminants. The study was conducted at a temperature of 25 °C and an initial pH of 3–6 with C_o 50 mg L^{-1}. The sorption uptake for the metal ions was faster in the initial stages and then slowed down, indicating the presence of non-reactive sites. The data showed that 94.6% Pb^{2+} and

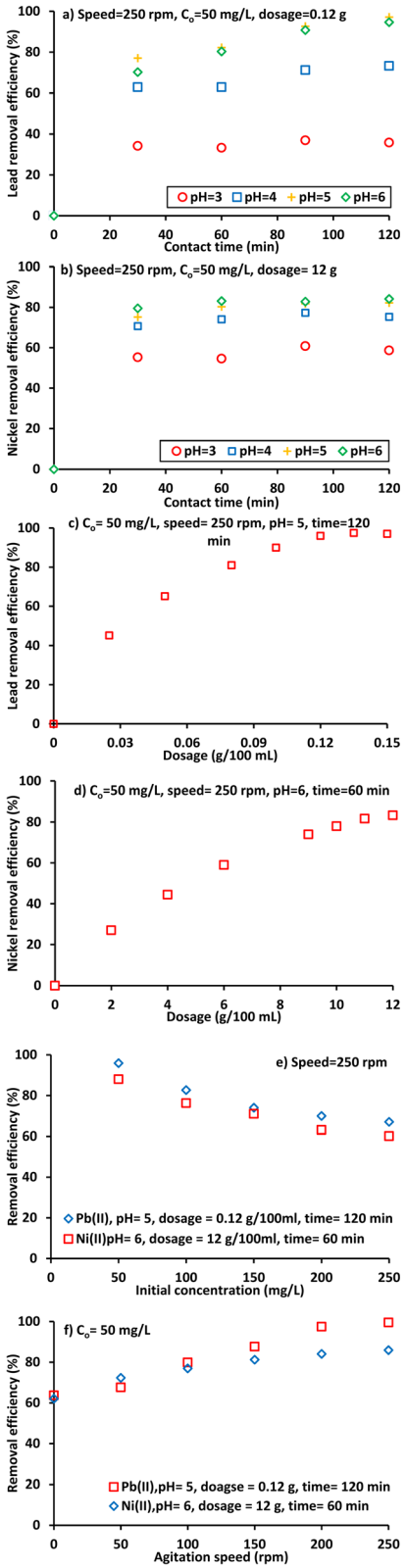

Fig. 2 Influences of operation factors on the removal efficiencies of lead and nickel ions on the clay reactive material.

83.1% Ni^{2+} were removed at 120 and 60 min respectively for an initial pH of 6. The pH had a potential impact on the removal process, with a pH of 5 being sufficient for maximum removal of lead ions and pH 6 for nickel ions. The best contact time for the next batch experiments was suggested to be within the range of the current study (60–180 min).

Results in Fig. 2(a) and (b) certify that the values of initial pH have had significant influence on the removal process and the pH of 5 was sufficient to achieve the maximum removal of lead ions while most species of nickel can be removed at pH = 6. Due to the high protonation at the acidic ambient, the sorption could considerably be reduced owing to the most probable competition induced between the cationic metal ions and the protons evolved at low pH.[37] However, the pH of aqueous solution was selected to be not greater than 7 to avoid the possibility of ions precipitation.[38]

The dependence of Pb^{2+} and Ni^{2+} sorption on clay amounts was investigated by taking different amounts of clay sorbent that must be within the restricted ranges illustrated in Fig. 2(c) and (d) and within the pre-adjusted batch experimental parameters to 100 mL solution at 25 °C, 50 mg L^{-1} initial concentration, 250 rpm agitation speed, for pH of 6, and 60 and 120 min time of contact for nickel and lead ions respectively. These figures show that the more clay sorbent present; the higher the removal efficiency is achieved and this is due to the presence of further reactive sorption sites. It seems that the best values of clay dosage were found to be 0.12 g/100 mL for Pb(II) and 12 g/100 mL for Ni(II).

The dependence of the removal efficiency of metal ions upon the initial concentration is elucidated through Fig. 2(e) wherein marginal decrease in the metal concentration was observed when increasing C_o up to 200 mg L^{-1} and this is an indication that is no more vacant sorption sites are available.[39] All the best experimental parameters investigated so far have been taken into consideration; besides, the influence of agitation speed has also been examined when varying speed from stationary up to 250 rpm. Fig. 2(f) showed that greater than 60% of lead and nickel had been removed onto Iraqi clay without agitation. The removal percentage has afterwards increased at higher speed to become over 85% at 250 rpm and this is due to the elimination of the resistant to mass transfer Nernst film covering the sorbent surface.

Sorption isotherms

Generally, an isothermal adsorption is an essential curve that describes the distribution of chemical at specific temperature in the aqueous and solid phases. Isotherms mentioned previously are used for representing the sorption data of lead and nickel. Fig. 3 and 4 present the plots of experimental results and their fitted lines. For each model using a linear plot *via* Microsoft Excel 2003 software, the determination coefficient (R^2) was calculated. It is evident that in comparison with other Pb^{2+} and Ni^{2+} isothermal models, the Langmuir was the best correlation of all. Accordingly, this model (with q_m and b = 137 mg g^{-1} & 0.049 L mg^{-1} for lead and 1.75 mg g^{-1} and 0.027 L mg^{-1} for nickel respectively) will be applied to represent the term of

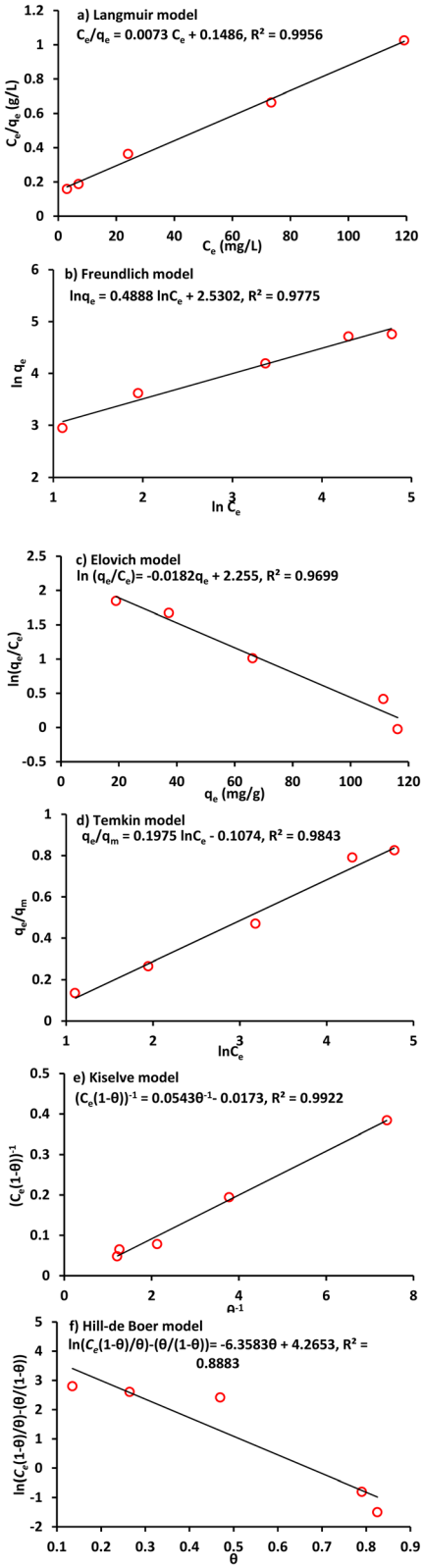

Fig. 3 Linear forms of isotherms for Pb^{2+} sorption onto clay (C_o = 50 mg L^{-1}, speed = 250 rpm, time = 120 min, pH = 5 and dosage = 0.12 g/100 mL).

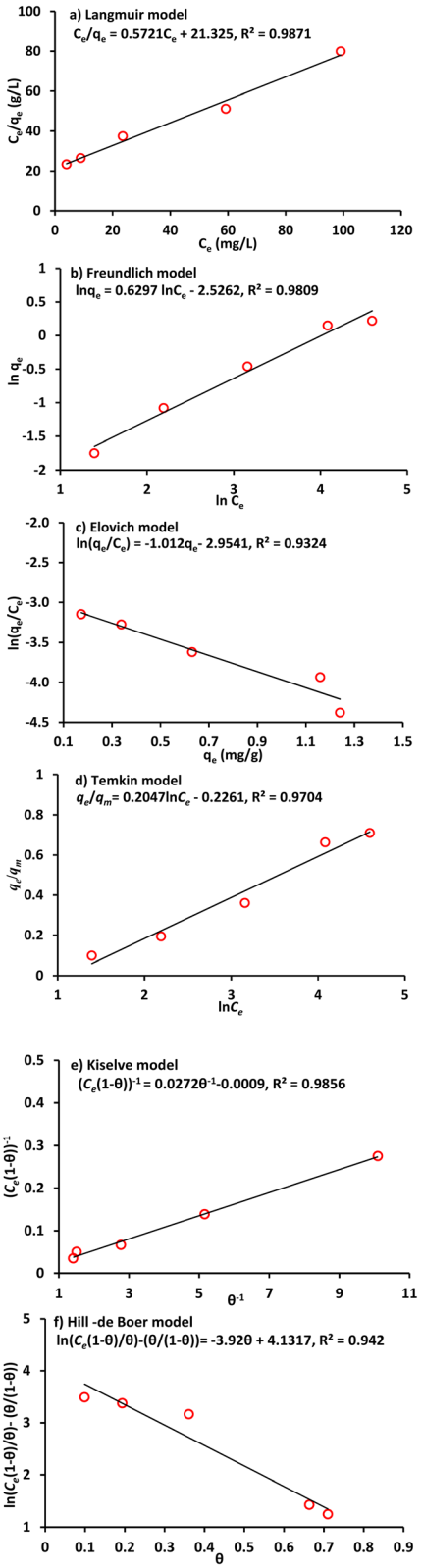

Fig. 4 Linear forms of isotherms for Ni^{2+} sorption onto clay (C_o = 50 mg L^{-1}, speed = 250 rpm, time = 60 min, pH = 6 and dosage = 12 g/100 mL).

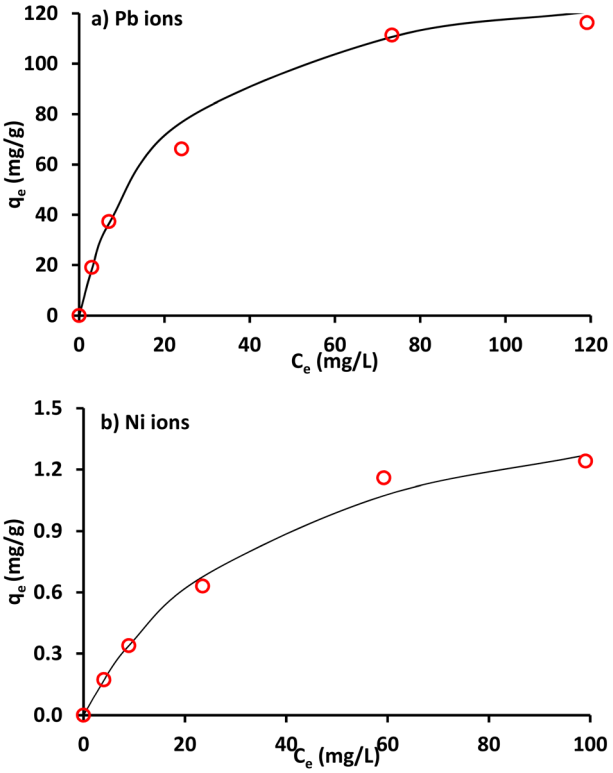

Fig. 5 Measurements of q_e in comparison with values obtained by Langmuir model for Pb^{2+} and Ni^{2+} removal by clay.

reaction in solute equation for metal migration in continuous mode operation. The sorbed quantities of metal ions were recalculated by using Langmuir parameters at different values of equilibrium concentrations (Fig. 5) to illustrate the concurrence between Langmuir graph and measurements; however, this concurrence was generally good for situation under consideration. In addition, lead has greater sorptive characteristic because its isotherm curve is higher up in this figure.[40]

Fourier transform infrared (FT-IR) analysis

This analysis is viewed as a type of direct method for the examination of sorption mechanisms by specifying the functional binding groups of Pb^{2+} or Ni^{2+}. Infrared samples of clay were studied using Shimadzu FT-IR, 8000 before and after the sorption of Pb^{2+} or Ni^{2+}. Fig. 6 depicts the spectral measurement within the range 400–4000 cm^{-1}. The shifts in the infrared frequencies (Table 1) support that Al–Al–Mg, Al–Al–OH, Al–OH–Mg, and Si–O–Mg were the bonds of the groups responsible for the sorption of metal ions under consideration onto clay.[41] The vibrations of the H_2O and Si–O groups can be affected by the octahedral and tetrahedral sheets produced by the adsorption of Pb^{2+} or Ni^{2+}. When compared to virgin clay, the patterns of the FT-IR for clay loaded with these ions revealed a shift in the water broad band. Replacement of alkaline metals with Pb^{2+} or Ni^{2+} ions for virgin clay may be the path for occurrence of adsorption process. A type of swelling clay known as montmorillonite contains hydrational water. The extent of clay hydration is based on the nature and type of inter-layer cations, temperature and its

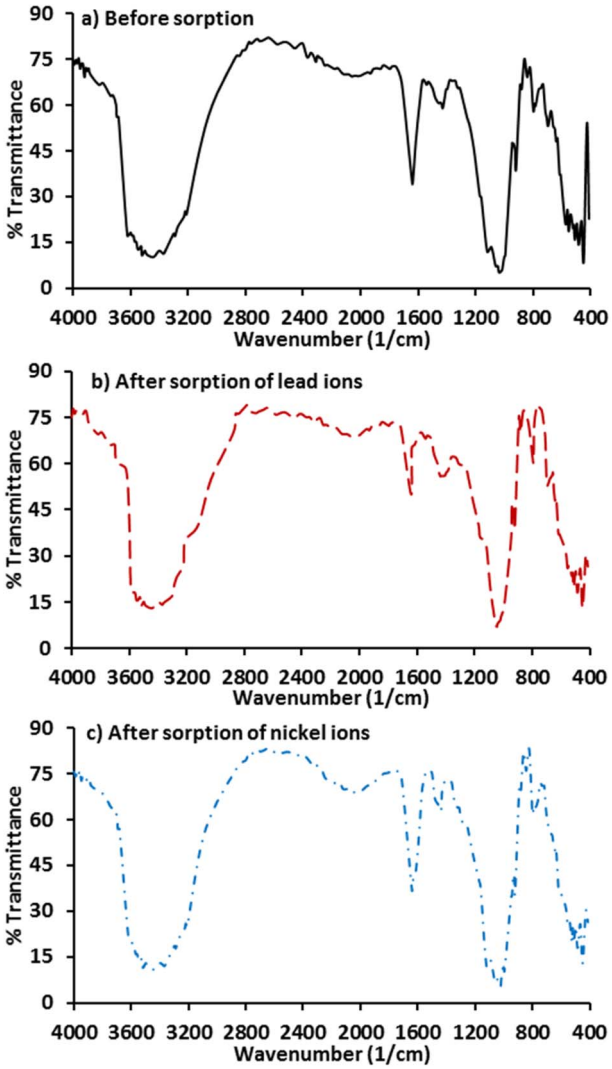

Fig. 6 FT-IR test for clay before and beyond loaded with ions of lead and nickel.

Table 1 Working groups enhanced the sorption of Pb^{2+} and Ni^{2+} onto Iraqi clay

Metal	Wavenumber (1/cm)	Type of bond
Pb^{2+}	3670	Al–Al–Mg
	955	Al–Al–OH
	851	Al–OH–Mg
	648	Si–O–Mg
Ni^{2+}	3621	Al–Al–OH
	916	Al–Al–OH
	788	Fe^{3+}–OH–Mg
	610	Si–O–Al

crystalline structure. Because, the state of hydration for montmorillonite can be reflected through the size of its inter-layer space. Clay's Mg^{2+} and Fe^{3+} replaced Si^{4+} in the montmorillonite's silicon–oxygen tetrahedron; lastly, the adsorption was the predominant process, as evidenced by the band shifts.

Table 2 Auxiliary conditions applied for modeling of two-dimensional solute transport and water flow through LPB and aquifer

Item	Parameter/location	Value
Sand aquifer	Porosity	0.46
	Hydraulic conductivity (m s^{-1})	2.2×10^{-5}
	Longitudinal dispersivity (m)	0.701
	Bulk density (kg m^{-3})	1390
LPB	Porosity	0.547
	Hydraulic conductivity (m s^{-1})	6.5×10^{-10}
	Bulk density (kg m^{-3})	1114
	Longitudinal dispersivity (m)	0.827
BCs-water flow	h (cm) – line source	5
	h (cm) – outlet side	Zero
	Zero flux/symmetry for other sides	—
BCs-metal transport	Conc. (mg L^{-1}) – line source	50
	Advective flux – outlet side	—
	No. flux/symmetry for other sides	—
IC-metal transport	Conc. at $t = 0$ for flow domain	Zero

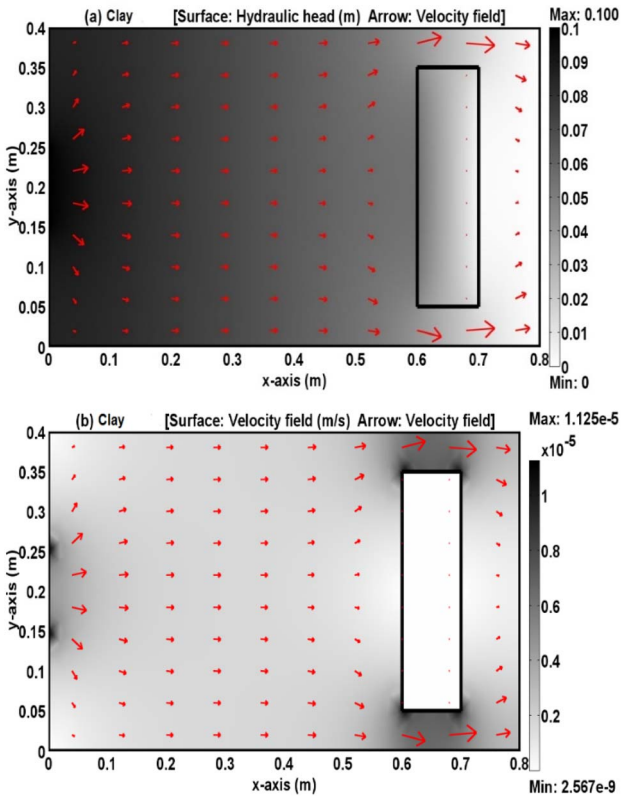

Fig. 7 Variation of flow characteristics through 2D sandy soil domain packed in the tank with existence of clay as plotted by COMSOL program for steady flow.

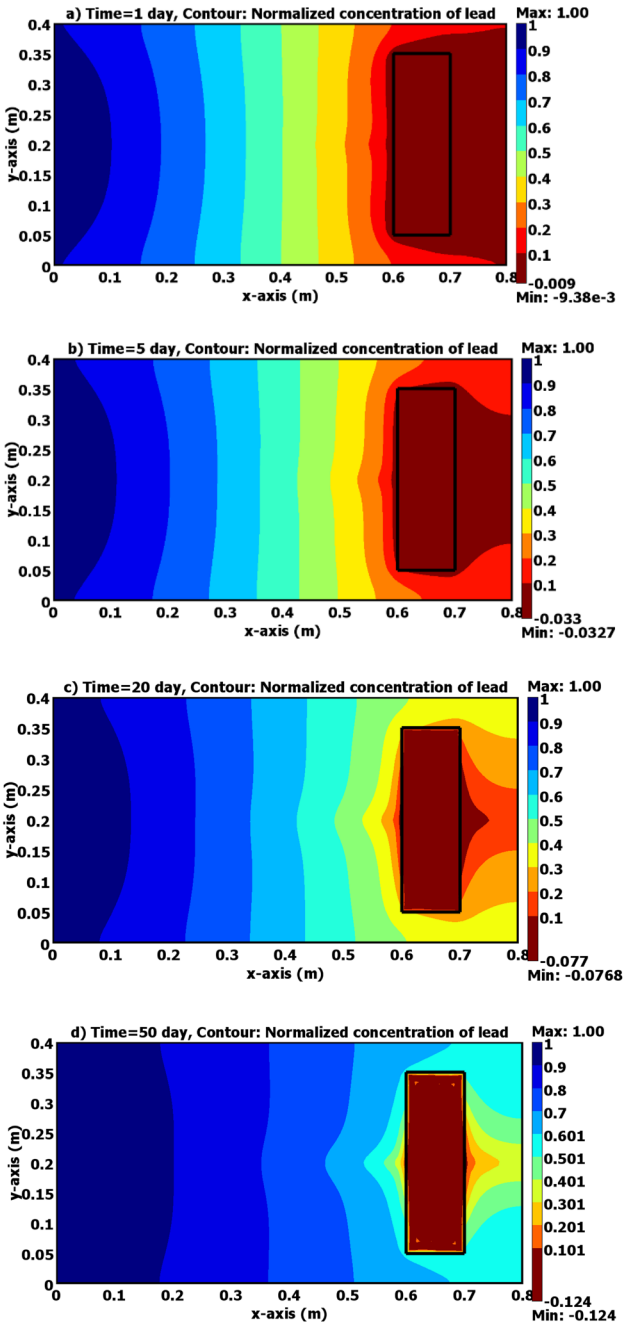

Fig. 8 Contours of (C/C_o) of lead through 2D sandy soil domain packed in the tank with existence of clay as plotted by COMSOL program for (a) 1, (b) 5, (c) 20, and (d) 50 days.

Contaminant transport through the aquifer and LPB

The time dependent partial differential equation (eqn (8)) is well representation for the contaminant spatial movement in the cartesian two-dimensions:

$$\frac{\partial}{\partial x}\left(K_x \frac{\partial h}{\partial x}\right) + \frac{\partial}{\partial y}\left(K_y \frac{\partial h}{\partial y}\right) = S_s \frac{\partial h}{\partial t} \quad (8)$$

where K is the hydraulic conductivity in any direction, h is the hydraulic head and S_s is the specific storage capacity which is the volume of water per unit of a porous saturated medium that has been storing or expelled because of compression of the solid structure of the medium and pore water per unit head change. Eqn (8) can numerically be solved by COMSOL software. If no head change with time at steady-status; the right hand side of eqn (8) tends to approach zero:

$$\frac{\partial}{\partial x}\left(K_x \frac{\partial h}{\partial x}\right) + \frac{\partial}{\partial y}\left(K_y \frac{\partial h}{\partial y}\right) = 0 \quad (9)$$

The advection–dispersion processes contribute to the contaminant propagation through the porous medium. Eqn (10) is the unsteady-state transient two-dimensional solute transport is outlined as a result of solute mass balance through porous medium:

$$D_x \frac{\partial^2 C}{\partial x^2} + D_y \frac{\partial^2 C}{\partial y^2} - V_x \frac{\partial C}{\partial x} = R \frac{\partial C}{\partial t} \quad (10)$$

where D is the dispersion coefficient, C is the solute concentration, R is the retardation factor which can be determined with aid of Langmuir model for reaction term:

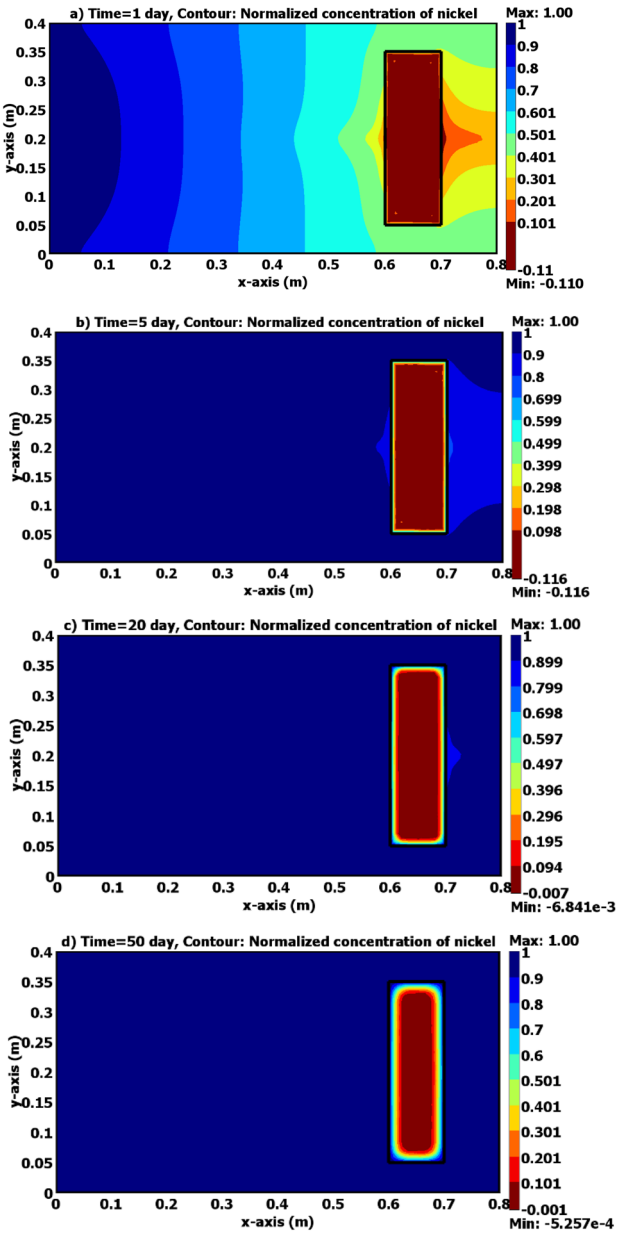

Fig. 9 Contours of (C/C_o) of lead through 2D sandy soil domain packed in the tank with existence of clay as plotted by COMSOL program for (a) 1, (b) 5, (c) 20, and (d) 50 days.

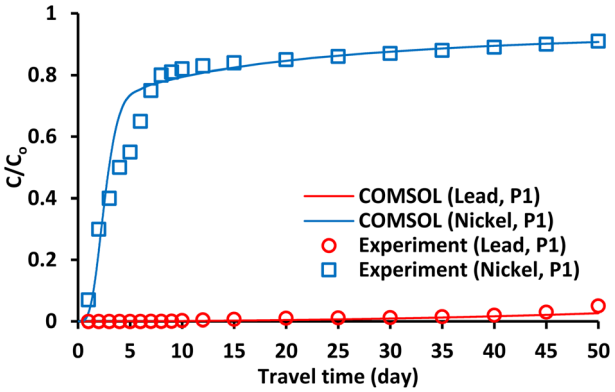

Fig. 10 Results of (C/C_o) of lead and nickel predicted by COMSOL program in comparison with measurements just beyond clay-LPB at P1.

$$R = 1 + \frac{\rho_b}{n}\left(\frac{q_m b}{(1+bC)^2}\right) \quad (11)$$

where ρ_b and n are the bulk density and porosity of packed bed respectively.

The 2D steady-state water flow and transient solute transport in a shallow aquifer plotted in Fig. 1 are carried out physically and simulated by the COMSOL package. The configuration model comprises 80 × 40 × 5 cm dimensions as well as a 10 cm line source. Table 2 reveals the system properties as well as the initial and boundary conditions (IC and BCs) for the solution of the solute transport equation by the COMSOL software package which determines the velocity distribution and metal ion concentrations in two dimensions. Fig. 7 reveals the COMSOL predictions of the two-dimensional hydraulic head and velocity distribution for the sandy soil zone as a result of the LPB impact on the groundwater flow.

Fig. 8 and 9 depict the normalized Pb^{2+} and Ni^{2+} content in the 2D sandy tank as predictable to COMSOL over various durations. Clearly, the down-gradient barrier in the source of contaminant significantly reduces advective transportation; furthermore, the advective direction is laterally near the barrier and downward gradients for a short distance tends to enlarge the plume width as the flat line extends across the barrier.[16,19,21,42,43] These figures certified that the clay barrier has high affinity towards contaminants and tend to retard the front of plum ions compared with nickel. Fig. 10 depicts a comparison between the measurements and predictions for the normalized metal concentrations in port P1 at the coordinates (0.7 m, 0.2 m) downstream the barrier. It is obvious that there appeared well agreement between the predicted and experimental results. However; it seems that the clay barrier has more ability for restricting of lead ions movement in comparison with nickel ones and this may result from difference in the affinity of clay towards these metals.[44]

Conclusions

The batch and continuous studies found that Iraqi clay is an effective material for retaining lead and nickel ions, and can be

used as a "LPB" to protect water resources from contamination. To achieve removal efficiencies of over 80%, the batch study determined the optimal parameters for the interaction of lead with Iraqi clay to be pH 5, 120 minutes of contact time, and a clay mass of 0.12 g/100 mL. For nickel, the optimal parameters were found to be pH 6, 60 minutes of contact time, a clay mass of 12 g/100 mL, and an agitation speed of 250 rpm at an initial concentration of 50 mg L^{-1}. Analysis of equilibrium sorption data using various isotherms showed that the Langmuir isotherm could accurately describe the data with an R^2 value of not less than 0.98. FT-IR testing identified the major contributors to metal ion uptake as aromatic, alcohol, alkyl halides, and alkane groups. The results suggest that LPB acts as an upstream and downstream barrier to prevent the advancement of contaminants. However, as subsurface water flows near the barrier, an advection process may spread the contaminants plume in the downstream direction.

Author contributions

Conceptualisation, A. A. H. Faisal, Z. A. A and O. A. H; methodology A. A. H. Faisal and W. H. H.; software, Z. A. A, K. H.; validation, A. A. H. Faisal and Z. A. A.; formal analysis, and investigation, N. A.—original draft preparation, O. A.-H, A. A. H, A. A. G. and N. A; writing—review and editing, W. H. H, A. A. H. Faisal and Z. A. A; supervision, K. H. and A. A. H. Faisal.

Conflicts of interest

The authors declare no conflict of interest.

Acknowledgements

We would like to gratefully acknowledge the technical support of Environmental Engineering Department/University of Baghdad provided during the present work. One of the authors (Ayman A. Ghfar) is grateful to the Researchers Supporting Project number (RSP2023R407), King Saud University, Riyadh, Saudi Arabia for the financial support.

References

1 H. Rashid and A. Faisal, Removal of dissolved trivalent chromium ions from contaminated wastewater using locally available raw scrap iron-aluminum waste, *Al-Khawarizmi Eng. J.*, 2019, **15**, 134–143.
2 R. Thiruvenkatachari, S. Vigneswaran and R. Naidu, Permeable reactive barrier for groundwater remediation, *J. Ind. Eng. Chem.*, 2008, **14**, 145–156.
3 A. A. H. Faisal and Z. T. Abd Ali, Using sewage sludge as a permeable reactive barrier for remediation of groundwater contaminated with lead and phenol, *Sep. Sci. Technol.*, 2017, **52**, 732–742.
4 G. Sharma, D. Pathania, M. Naushad and N. C. Kothiyal, Fabrication, characterization and antimicrobial activity of polyaniline Th(IV) tungstomolybdophosphate nanocomposite material: Efficient removal of toxic metal ions from water, *Chem. Eng. J.*, 2014, **251**, 413–421.
5 M. Naushad, S. Vasudevan, G. Sharma, A. Kumar and Z. A. Alothman, Adsorption kinetics, isotherms, and thermodynamic studies for Hg2+ adsorption from aqueous medium using alizarin red-S-loaded amberlite IRA-400 resin, *Desalin. Water Treat.*, 2016, **57**, 18551–18559.
6 X. H. Zhang, Remediation techniques for soil and groundwater, *Point sources Pollut. local Eff. its Control - Vol II*, 2009, p. 514.
7 M. Naushad, A. Mittal, M. Rathore and V. Gupta, Ion-exchange kinetic studies for Cd(II), Co(II), Cu(II), and Pb(II) metal ions over a composite cation exchanger, *Desalin. Water Treat.*, 2015, **54**, 2883–2890.
8 M. Naushad and Z. A. Alothman, Separation of toxic Pb2+ metal from aqueous solution using strongly acidic cation-exchange resin: analytical applications for the removal of metal ions from pharmaceutical formulation, *Desalin. Water Treat.*, 2015, **53**, 2158–2166.
9 G. Sharma and M. Naushad, Adsorptive removal of noxious cadmium ions from aqueous medium using activated carbon/zirconium oxide composite: Isotherm and kinetic modelling, *J. Mol. Liq.*, 2020, **310**, 113025.
10 W. Hassan, A. Faisal, E. Abed, N. Al-Ansari and B. Saleh, New composite sorbent for removal of sulfate ions from simulated and real groundwater in the batch and continuous tests, *Molecules*, 2021, **26**, 4356.
11 J. Kim and M. Y. Corapcioglu, Modeling dissolution and volatilization of LNAPL sources migrating on the groundwater table, *J. Contam. Hydrol.*, 2003, **65**, 137–158.
12 A. A. H. Faisal and Z. A. Hmood, Groundwater protection from cadmium contamination by zeolite permeable reactive barrier, *Desalin. Water Treat.*, 2015, **53**, 1377–1386.
13 A. H. Sulaymon, A. A. H. Faisal and Q. M. Khaliefa, Cement kiln dust (CKD)-filter sand permeable reactive barrier for the removal of Cu(II) and Zn(II) from simulated acidic groundwater, *J. Hazard. Mater.*, 2015, **297**, 160–172.
14 A. A. H. Faisal and M. D. Ahmed, Removal of copper ions from contaminated groundwater using waste foundry sand as permeable reactive barrier, *Int. J. Environ. Sci. Technol.*, 2015, **12**, 2613–2622.
15 P. Bayer, M. Finkel and G. Teutsch, Combining Pump-and-Treat and Physical Barriers for Contaminant Plume Control, *Groundwater*, 2004, **42**, 856–867.
16 E. I. Anderson and E. Mesa, The effects of vertical barrier walls on the hydraulic control of contaminated groundwater, *Adv. Water Resour.*, 2006, **29**, 89–98.
17 M. M. Ibreesam and A. A. H. Faisal, Influence of low permeable barrier on the migration of cadmium ions in the subsurface medium, *Plant Arch*, 2020, **20**, 384–389.
18 A. A. H. Faisal, Z. A. Al-Ridah, L. A. Naji, M. Naushad and H. A. El-Serehy, Waste foundry sand as permeable and low permeable barrier for restriction of the propagation of lead and nickel ions in groundwater, *J. Chem.*, 2020, **2020**, 1–13.
19 A. I. Bezzar, D. François and F. Ghomari, Geochemical study of clays used as barriers in landfills, *C. R. Geosci.*, 2010, **342**, 695–700.

20 A. A. H. Faisal, W. M. S. Kassim and T. K. Hussein, Influence of clay lens on migration of light nonaqueous phase liquid in unsaturated zone, *J. Environ. Eng.*, 2011, **137**, 9–14.
21 T. Sarabian and M. T. Rayhani, Hydration of geosynthetic clay liners from clay subsoil under simulated field conditions, *Waste Manage.*, 2013, **33**, 67–73.
22 A. A. H. Faisal, *et al.*, COMSOL multiphysics 3.5a package for simulating the cadmium transport in the sand bed-bentonite low permeable barrier, *J. King Saud Univ., Sci.*, 2020, **32**, 1944–1952.
23 M. Naushad, Surfactant assisted nano-composite cation exchanger: Development, characterization and applications for the removal of toxic Pb2+ from aqueous medium, *Chem. Eng. J.*, 2014, **235**, 100–108.
24 M. Naushad, Z. A. Alothman, M. R. Awual, M. M. Alam and G. E. Eldesoky, Adsorption kinetics, isotherms, and thermodynamic studies for the adsorption of Pb2+ and Hg2+ metal ions from aqueous medium using Ti(IV) iodovanadate cation exchanger, *Ionics*, 2015, **21**, 2237–2245.
25 G. Sharma, *et al.*, Utilization of Ag2O–Al2O3–ZrO2 decorated onto rGO as adsorbent for the removal of Congo red from aqueous solution, *Environ. Res.*, 2021, **197**, 111179.
26 G. Sharma, *et al.*, Adsorptional-photocatalytic removal of fast sulphon black dye by using chitin-cl-poly(itaconic acid-co-acrylamide)/zirconium tungstate nanocomposite hydrogel, *J. Hazard. Mater.*, 2021, **416**, 125714.
27 D. N. Ahmed, A. A. H. Faisal, S. H. Jassam, L. A. Naji and M. Naushad, Kinetic Model for pH Variation Resulted from Interaction of Aqueous Solution Contaminated with Nickel Ions and Cement Kiln Dust, *J. Chem.*, 2020, **2020**, 1–11.
28 A. A. H. Faisal, S. S. Alquzweeni, L. A. Naji and M. Naushad, Predominant mechanisms in the treatment of wastewater due to interaction of benzaldehyde and iron slag byproduct, *Int. J. Environ. Res. Public Health*, 2020, **17**, DOI: **10.3390/ijerph17010226**.
29 A. A. H. Faisal, S. F. A. Al-Wakel, H. A. Assi, L. A. Naji and M. Naushad, Waterworks sludge-filter sand permeable reactive barrier for removal of toxic lead ions from contaminated groundwater, *J. Water Process. Eng.*, 2020, **33**, 101112.
30 M. Alshammari, *et al.*, Synthesis of a Novel Composite Sorbent Coated with Siderite Nanoparticles and its Application for Remediation of Water Contaminated with Congo Red Dye, *Int. J. Environ. Res.*, 2020, **14**, 177–191.
31 M. F. Al Juboury, *et al.*, Synthesis of composite sorbent for the treatment of aqueous solutions contaminated with methylene blue dye, *Water Sci. Technol.*, 2020, **7**, 1494–1506.
32 D. N. Ahmed, L. A. Naji, A. A. H. Faisal, N. Al-Ansari and M. Naushad, Waste foundry sand/MgFe-layered double hydroxides composite material for efficient removal of Congo red dye from aqueous solution, *Sci. Rep.*, 2020, **10**, 2042.
33 Y. S. Ho, J. F. Porter and G. McKay, Equilibrium isotherm studies for the sorption of divalent metal ions onto peat: Copper, nickel and lead single component systems, *Water, Air, Soil Pollut.*, 2002, **141**, 1–33.
34 O. Hamdaoui and E. Naffrechoux, Modeling of adsorption isotherms of phenol and chlorophenols onto granular activated carbon Part II. Models with more than two parameters, *J. Hazard. Mater.*, 2007, **147**, 401–411.
35 K. Y. Foo and B. H. Hameed, Insights into the modeling of adsorption isotherm systems, *Chem. Eng. J.*, 2010, **156**, 2–10.
36 S. Wang, Z. Nan, Y. Li and Z. Zhao, The chemical bonding of copper ions on kaolin from Suzhou, *Desalination*, 2009, **249**, 991–995.
37 S. U. Kurnaz and H. Buyukgungor, Assessment of various biomasses in the removal of phenol from aqueous solutions, *J. Microb. Biochem. Technol.*, 2009, **1**, 47–50.
38 A. H. Sulaymon, M. Y. Abdul-Ahad and R. A. Mahmood, Removal of Water Turbidity by Different Coagulants, *J. Eng.*, 2013, **19**, 1566–1575.
39 R. Qadeer and A. H. Rehan, A study of the adsorption of phenol by activated carbon from aqueous solutions, *Turk. J. Chem.*, 2002, **26**, 357–362.
40 A. Faisal and M. Ahmed, Remediation of groundwater contaminated with copper ions by waste foundry sand permeable barrier, *J. Eng.*, 2014, **20**, 62–77.
41 K. M. Doke, M. Yusufi, R. D. Joseph and E. M. Khan, Biosorption of hexavalent chromium onto wood apple shell: equilibrium, kinetic and thermodynamic studies, *Desalin. Water Treat.*, 2012, **50**, 170–179.
42 A. Tuncan and M. Inanc Onur, Design of Landfill Liner for Boron Mine Waste Water, *Int. J. Waste Resour.*, 2016, **6**, 207.
43 P. T. Harte, L. F. Konikow and G. Z. Hornberger, Simulation of solute transport across low-permeability barrier walls, *J. Contam. Hydrol.*, 2006, **85**, 247–270.
44 M. M. Ibreesam and A. A. H. Faisal, Using Cement Kiln Dust as Low Permeable Barrier for Restriction the Propagation of Cadmium Ions Towards the Water Resources, *Iraqi J. Agric. Sci.*, 2020, **51**, 1581–1592.